活断層・古地震研究報告，No. 4, p. 243-264, 2004

Rupture geometry and multi-segment rupture of the November 2001 earthquake in the Kunlun fault system, northern Tibet, China

Bihong Fu[1], Yasuo Awata[2], Jianguo Du[3] and Wengui He[4]

[1, 2]Active Fault Research Center, GSJ/AIST (bihongfu-fu@aist.go.jp, awata-y@aist.go.jp)
[3]Institute of Earthquake Science, CEA (jgdu@163.com)
[4]Lanzhou Institute of Seismology, CEA (hewg@public.lz.gs.cn)

Abstract: We document the spatial distribution and geometry of surface rupture zone produced by the 2001 M_w 7.8 Kunlun earthquake, based on high-resolution satellite images combined with the field measurements. Our results show that the 2001 surface rupture zone can be divided into five segments according to the geometry of surface rupture. They are the Sun Lake, Buka Daban-Hongshui River, Kusai Lake, Hubei Peak and Kunlun Pass segments from west to east. These segments, varying from 55 to 130 km in length, are separated by step-overs or bends. The Sun Lake segment extends about 65 km with a strike of N45º-75ºW (between 90º05'E-90º50'E) along the previously unrecognized West Sun Lake fault. A gap about 30 km long exists between the Sun Lake and Buka Daban Peak where no obvious surface ruptures can be observed either from the satellite images or the field observations. The Buka Daban-Hongshui River, Kusai Lake, Hubei Peak and Kunlun Pass segments run about 365 km striking N75º-85ºW along the southern slope of the Kunlun Mountains (between 91º07'E-94º58'E). This segmentation of the 2001 surface rupture zone is well correlated with the pattern of slip distribution measured in the field; that is, the abrupt changes of slip distribution occur at segment boundaries. Detailed mapping suggest that these five first-order segments can be divided into over 20 second-order segments with the length of 10-30 km, linked by small-scale step-overs or bends. We re-measure the total rupture length produced by the 2001 Kunlun earthquake based on the high precision mapping. It shows that the total length is about 430 km (excluding the 30 km long gap), which is the longest among the intraplate earthquakes ever reported worldwide. On the basis of rupture geometry and segmentation, and slip distribution along the surface rupture zone, we suggest a multiple bilateral rupture propagation model. Our model shows that the faulting process of the 2001 Kunlun earthquake is quite complex, which consists of multiple westward and eastward rupture propagations, and interaction of these bilateral rupture processes. It is much more complex than the simple unilateral rupture process suggested by previous studies.

Keywords: satellite imagery; surface rupture; geometric feature; multi-segment earthquake; step-over and bend; strike-slip faulting; bilateral propagation; great intraplate earthquake; India-Eurasia collision; northern Tibet.

1. Introduction

Most large earthquakes in historical time ruptured only a part of long active faults (Ambraseys, 1970; Barka and Kadinsky-Cade, 1988; Stein *et al*., 1997). Surface ruptures often terminate at geometric or structural changes in the fault zone (Allen, 1968; Barka and Kadinsky-Cade, 1988). Changes in fault strength, geometry, and slip distribution may result in rupture segmentation (e.g., Ward, 1997; Zhang *et al*., 1999; Awata *et al*., 2001). This segmentation is manifested by consistent spatial and temporal rupture behavior that may be used to forecast the timing and magnitude of future events (e.g., Schwartz and Coppersmith, 1984; Van der Woerd *et al*., 1998).

The Kunlun earthquake, of moment magnitude (M_w) 7.8, occurred on 14 November 2001 along the Kusai Lake fault of the Kunlun fault system, northern Tibet (Fig. 1; Lin *et al*., 2002). Immediately after the earthquake, several multidisciplinary research teams from China Seismological Bureau (CSB), and Institute of Geomechanics, Chinese Academy of Geological Sciences, and Shizuoka University (Japan) conducted field investigations on deformational characteristics of surface rupture zone and engineering damage. The preliminary results show that the Kunlun earthquake produced a long surface rupture zone with a length of ~350 km (CSB, 2002; 2003; Dang and Wang, 2002; Xu *et al*., 2002) or ~400 km (Lin *et al*., 2002; Fu and Lin, 2003). The typical lateral slip is 3 to 7 m (Xu *et al.,* 2002; Fu *et al*., 2003; 2004a), and the largest one is up to 16.3 m (Lin *et al*., 2002). Field investigations also indicate that the surface rupture zone is composed of distinct shear faults, extensional cracks, mole tracks, and pull-apart sag ponds.

The width of surface rupture zone ranges from several meters to 1000 m, generally from 5 m to 50 m (Fu *et al.*, 2003, 2004a). This earthquake also triggered avalanches of snow and glacial ice and caused slight damage to the base of the Qinghai-Tibet railway and road between Golmud and Lhasa. Ground shaking collapsed temporary housing for workers on the railway (Fu *et al.*, 2003).

Up to now, there is no detailed report on the geometry of surface rupture zone. The surface rupture occurred on the Kunlun Mountains with an elevation over 4500 m, where detailed field mapping of the surface rupture is difficult. Thus, it is difficult to document the entire geometry of surface rupture zone from the field mapping.

In this study, we shall document geometric and geomorphic features of the 2001 Kunlun surface rupture zone based on detailed analysis of high-resolution satellite images combined with the data obtained from the field investigations. We shall also discuss rupture segmentation and rupture processes related to the 2001 seismic event.

2. Data and methods

Satellite remote sensing technique has been demonstrated as a powerful tool for mapping coseismic deformational features caused by large earthquakes (e.g., Fu and Lin, 2003; Wright *et al.*, 2004). Satellite remote sensing data acquired by the American Landsat Thematic Mapper (TM) and Enhanced Thematic Mapper (ETM), the French Systeme Probatoire de 1' Observation de 1a Terre (SPOT) High Resolution Visible (HRV) sensor, and the Japanese Advanced Spaceborne Thermal Emission and Reflection Radiometer (ASTER) currently provide important sources for earth surface mapping. Landsat TM/ETM have 15 to 30 m ground resolution, whereas ground resolutions of SPOT HRV Panchromatic (PAN) and ASTER data in Visible and Near Infrared (VNIR) region are 10 m and 15 m, respectively. Pre-earthquake (during 1998 to 2000) and post-earthquake (from late November, 2001 to May, 2002) satellite remote sensing data covering the western part of the Kunlun fault system are used in this study. The rupture zone can not be distinguished clearly from post-earthquake satellite images obtained after June 2002 because the surface rupture zone was eroded by summer snow and ice meltwaters. In addition, to analyze geometry of the 2001 surface rupture in detail we use post-earthquake American IKONOS data with 1 m resolution for post-earthquake period for some key regions.

These multi-source satellite remote sensing data were geometrically corrected and processed using ER-Mapper. Image mosaic, contrast stretch and band composition were used to enhance imagery feature of the surface rupture zone. Above-mentioned satellite remote sensing data provide an excellent view of the 2001 Kunlun earthquake surface rupture.

Satellite images at different scales (1/5,000 to 1/100,000) are used to interpret the geometric and geomorphic features of the 2001 rupture zone. Moreover, we carried out the field investigation several times along the surface rupture zone to obtain detailed deformational and geometric features of the surface rupture zone.

3. Late Quaternary activity and seismicity of the Kunlun fault system

The Tibetan Plateau is one of the most imposing topographic features on the earth surface (Fig. 1a), having a mean elevation of ~4500 m, which was resulted from India-Eurasia collision (Molnar and Tapponnier, 1975; 1978; Peltzer *et al.*, 1989). The E-W to WNW-ESE striking Kunlun fault system, extending about 1600 km between 86ºE to 105ºE, is one of the largest strike-slip faults in the northern Tibet, China (Molnar and Tapponnier, 1975; Van der Woerd *et al.*, 1998; SBPQ, 1999). As a major strike-slip fault, it plays an important role in the eastward extrusion of Tibet plateau accommodate to northeastward shortening caused by the India-Eurasia convergence (Avouac and Tapponnier, 1993; Tapponnier *et al.*, 2001). The main trace of the Kunlun fault system may be roughly divided into six principal faults, each 150-270 km long, on basis of the geometry of fault trace and structural assemblage (Fig. 1b; Van der Woerd *et al.*, 1998). The left-lateral strike-slip faulting of the Kunlun fault may have initiated since the early Pliocene or early Pleistocene (Kidd and Molnar, 1988; Fu and Awata, 2004). Analyses of satellite images, cosmogenic surface dating and radiocarbon dating and trench surveys suggested that the Kunlun fault is an active left-lateral strike-slip fault with an average slip rate of 10-20 mm/yr in the Quaternary (Kidd and Molnar, 1988); or 11.5 ± 2 mm/yr in the past 40 kyr (Zhao, 1996; Van der Woerd *et al.*, 1998; 2000).

Three large earthquakes (M > 7.0) including the 14 November 2001 M_w 7.8 Kunlun earthquake occurred along the Kunlun fault system during the last 100 years. The 18 November 1997 Manyi earthquake with M_w 7.6 broke the western-most 170-km-long Manyi fault between 86º30'E and 88º30'E (Fig. 1b). Maximum left-lateral displacement is ~7 m for the Manyi earthquake as revealed by synthetic aperture radar (SAR) interferometry (Peltzer *et al.*, 1999). The 1937 M_s 7.5 Tuosuo Lake earthquake produced rupture zone about 300-km-long between 96ºE and 99ºE on the Tuosuo Lake fault with a maximum left-lateral offset of 6-7 m (Jia *et al.*, 1988; Fig. 1b). No historical record of earthquakes had been reported along the Kusai Lake and Xidatan-Dongdatan faults although there are geomorphic features associated with seismic activities (Kidd and Molnar, 1988; Van der Woerd *et al.*, 1998; 2000). Based on the trenching survey, it has been inferred that recurrence interval of great earthquakes in the Xidatan-Dongdatan fault is 850 ± 200 yr with a characteristic slip of 10 ± 2 m (Zhao, 1996; Van der Woerd *et al.*, 1998; 2000; 2002).

4. Geometry and segmentation of the 2001 surface rupture zone

In the satellite image, the trace of Kusai Lake and

Kunlun Pass faults exhibit striking lineaments (Fig. 2a). The 2001 surface rupture zone distributes mostly along the pre-existing Kusai Lake and Kunlun Pass faults. We can divide the surface rupture zone into five first-order segments according to their geometric and structural features (Fig. 2b). They are the Sun Lake, Buka Daban-Hongshui River, Kusai Lake, Hubei Peak, and Kunlaun Pass segments from west to east, respectively. These first order segments, each 55 to 130 km long, are linked by 5 to 30 km long and 1 to 10 km wide step-overs or bends (Figs. 3, 6, 8a, 9, 10a, 12, 13). The detailed geometry of each segment is summarized as follows.

4.1 The Sun Lake Segment

The Sun Lake segment extends ~65 km between the Kushuiwan Lake (90º05'E) and east bank of the Sun Lake (90º50'E, Fig. 3). This segment can be further divided into four second-order segments, each 10 to 20 km long (Fig. 3b). It is the westernmost part of the 2001 November rupture zone (Zhao *et al.*, 2002) and strikes N40º-75ºW (Fig. 3). Typical lateral offset is 1 to 3 m as observed in the field (Zhao *et al.*, 2002). At the westernmost termination of the Sun Lake segment, some N70º-75ºW striking fissures and a N10ºW extending pressure ridge occurred in the frozen surface of the Kushuiwan Lake (Fig. 4a). On the east bank of the Kushuiwan Lake, two distinctive surface ruptures appear right-stepping pattern (Fig. 4a). The ruptures show a right-stepping en echelon arrangement in the central part of the Sun Lake segment. Eastward to the south of Peace Island, rupture zone splays into two distinctive ruptures (Fig. 3b). The southern branch runs about 3 km striking N45ºW, and northern branch continuously extends towards the Sun Lake with a strike of N65ºW (Figs. 4b and 5a). Large-scale IKONOS image shows that the third-order rupture segments (a, b, c, d, e, f, and g in Fig. 5a), each several hundreds meters to 2 km long, display a typical right-stepping en echelon pattern (Fig. 5a). In the field, the striking rupture zone occurs on the late Quaternary alluvial fans (Fig. 5b). Farther east to the west of the Sun Lake, three major ruptures developed in the frozen surface of the Sun Lake, which display as a tail pattern (Figs. 3b and 4b). These ruptures terminate on the eastern bank of the Sun Lake near 90º50'E (Fig. 3b). There is an about 30 km long gap between the Sun Lake and Buka Daban-Hongshui River segments, which display a left-stepping pattern (Figs. 2b and 3b). No obvious surface ruptures can be observed from the satellite images or field investigations. It may be a large unbroken barrier between the Sun Lake and Buka Daban-Honshui River rupture segments, where the step-over shows a large pull-apart basin (Fig. 3).

4.2 The Buka Daban -Hongshui River Segment

The trace of the Buka Daban-Hongshui River segment runs 110 km between the southeast Buka Daban Peak (91º07'E) and Hongshui River (92º18'E) with a strike of N75º-80ºW (Fig. 6). In the westernmost part of this segment, the rupture zone trends N45ºE and three left-stepping en-echelon arranging ruptures display a horse-tail pattern occurred on the moraine deposits on the southeast of the Buka Daban Peak (Figs. 6b and 7a). The IKONOS image exhibits the left-stepping geometry of major rupture zone, and the stream across the rupture zone is displaced left-laterally (Fig. 7b). Northeastward, the rupture bends into N80ºW (Fig. 6b). The Buka Daban-Hongshui River segment is further divided into 5 to 6 second-order segments, each 20-30 km long, interconnected by small-scale bends or step-overs (Fig. 6b). These small bends or step-overs, 1-3 km long and several hundreds meters wide, appear as the pressure-ridges on satellite image (Fig. 6a).

4.3 The Kusai Lake Segment

To the east of the Hongshui River, the rupture zone is called the Kusai Lake segment (Fig. 2b). There is a large step-over, ~10 km long and 1 km wide, between the Buka Daban-Hongshui River and Kusai Lake segments (Figs. 6b and 8a). The IKONOS image clearly shows that the ruptures consist of third-order segments, each several hundreds meters long, which are linked by small step-overs or bends (Fig. 8b). The pressure ridges are formed in these small-scale bends or step-overs (Fig. 8b). The Kusai Lake segment extends 55 km between 92º15'E and 92º48'E. This segment also can be further divided into five second-order segments by small-scale step-overs or bends (Fig. 9b). There are large-scale half-graben and pressure ridges, several kilometers long and several hundreds meters wide, linking these second-order segments (Fig. 9b). A segment boundary is just located on the northeast of Kusai Lake (Fig. 9b), where the ruptures display a complex geometry, appearing flat-lying Y-shape pattern (Fig. 10a). In the field, a striking rupture zone passes through northeast of the Kusai Lake (Fig. 10b).

4.4 The Hubei Peak Segment

The Hubei Peak segment distributes to the south of the Kunlun range, where several ice-capped high peaks stand over 5500 m. The length of this segment is about 70 km with a strike of N75º-85ºW between 92º48'E and 93º40'E (Fig. 9b). The rupture zone cut the pre-Quaternary basement rocks and Quaternary fluvial fans (Fig. 9b). Again, the Hubei Peak segment is divided into 5 to 6 second-order segments, each 10 to 30 km long (Fig. 9b). The small step-overs and bends, 1-3 km long and several hundreds meters wide, link those second-order segments (Fig. 11). To the east of this segment, the rupture zone consists of several sub-parallel ruptures with several hundreds meters separation (Fig. 9b), where the widest surface deformation zone was observed in the field (Lin *et al.*, 2002; Xu *et al.*, 2002). To the east of 93º30'E, the rupture zone splays into two branches: the northern one extends along the pre-existing Xidatan-Dongtatan fault of the Kunlun fault system, and it terminates near 93º40'E, whereas the southern branch continuously runs eastward (Fig. 9b). These two splaying ruptures appear as a left step-over, which forms a boundary between the Hubei Peak and Kunlun Pass segments (Figs. 12 and 13).

4.5 The Kunlun Pass Segment

The trace of the Kunlun Pass segment runs mostly along the pre-existing Kunlun Pass fault, extending more than 130 km in length between 93º35'E and 94º58'E (Fig. 13). This segment can be also separated into 6 to 7 second-order segments, 10-30 km long (Fig. 13 b). The surface rupture starts at south of 5933 m high peak, passes through the north of the Kunlun Pass, and continues to farther east. On the southern slope of Yuzhu Peak, the rupture zone runs across the modern glaciers (Fig. 13). Detailed geometry of the eastern part of the Kunlun Pass segment can be clearly observed in the large-scale post-earthquake SPOT image (Fig. 14a). Near the easternmost end of this segment, the rupture zone splays into two major zones at point B, which display a flat-lying Y-shape pattern as shown on the SPOT image (Fig. 14a). The northern one extends straightly eastward, and terminates near 94º55'E (point C in Fig. 14a). The southern one bends southeastward and appears as a horse-tail pattern (Fig. 14a). Finally, the surface rupture zone disappears near 94º58'E (point E in Fig. 14a). At the easternmost end of the Kunlun Pass segment, the ruptures consist of the right-stepping cracks with a strike of N60º-65ºE as observed in the field (Fig. 14b).

5. Discussion

5.1 Linkage among segment geometry, slip distribution and rupture process

It is a timely topic how to link the relations among segment geometry, surface displacements, and rupture propagation process of the long seismogenic faults (e.g., Schultz, 1999; Phillips *et al*., 2003). Our results show that the surface rupture zone, produced by the 2001 M_w 7.8 Kunlun earthquake, has a multi-segment pattern as described in the section 4 (Fig. 15a). The surface rupture zone is geometrically segmented at a variety of scales (Figs. 2b, 3b, 6b, 9b, and 13b). It can be divided into five first-order segments, individual segment length varying 55 km to 130 km. These first-order segments are separated by the step-overs 5-30 km long and 1-10 km wide or bends (Fig. 15a). Meanwhile, these first-order surface rupture segments are subdivided into over 20 second-order segments of 10 to 30 km long by smaller step-overs or bends (Figs. 3, 6, 9 and 13). Moreover, even smaller-scale third-order segments, each several hundreds meters to 3 km long, can be identified either from high-resolution satellite images (Figs. 5a, 7b and 8b) or field observations (Fu *et al*., 2003). A number of studies have demonstrated that faults are geometrically and mechanically segmented at variety of scales (e.g., Allen, 1968; Allen *et al*., 1991; Wallace, 1970; 1990). For example, the number of segments identified for the San Andreas fault ranges from 4 to 984 (Allen, 1968; Wallace, 1970). As explained by Schwartz and Sibson (1989), segments may represent the repeated coseismic rupture during a single event on a long fault with tens to hundreds of kilometers, or they may represent a part of a rupture associated with an individual faulting event and only a few kilometers long. Similarly, the surface rupture segments with different scales might be products of rupture events or sub-events with different scales (e.g., DePolo *et al*., 1991; Awata *et al*., 2001).

Our mapping also exhibits that step-overs or bends with different scales exist at segment boundaries (Figs. 3b, 4, 5a, 6b, 8, 9b, 10a, 11, 12 and 13b). These step-overs and bends are very important features that control the process of rupture initiation, propagation and termination (e.g., Segall and Pollard, 1980; King and Nabelek, 1985; Zhang *et al*., 1999). They not only reflect structural and geomorphic changes of fault geometry on the surface, but also represent variations of mechanical fault movement at depth (e.g., Schwartz and Coppersmith, 1984; Ward, 1997; Sugiyama *et al*., 2002). Formation mechanism of step-over and bend and their geomorphic features had been noted by a number of previous studies (e.g., King, 1986; Dooley and McClay, 1997; McClay and Bonora, 2001). At these segment boundaries, the slip distribution along the rupture zone shows an abrupt change (Fig. 15b). Thus, multi-segment geometry pattern of the surface rupture zone might record the processes of fault nucleation, slip, linkage and propagation (Schultz, 1999; Aydin and Kalafat, 2002).

Comparing the analysis of geometry of the surface rupture zone and pattern of slip distribution with the seismic data, we suggest a model to explain the faulting processes or rupture propagation during the 2001 November earthquake (Fig. 15c). As indicated by seismic waveform inversion, the 2001 M_w 7.8 Kunlun earthquake may consist of three major sub-events (Lin *et al*., 2003; Xu and Chen, 2004). Our model shows that the 2001 Kunlun seismic event has a complex multiple rupture process (Fig. 15c). In our model, the rupture started near 90º30'E, which is consistent with the epicenter location reported by the USGS (Fig. 15b), and it propagated bilaterally eastward and westward. Westward rupture terminated on the Kushuiwan Lake near 90º05'E (Fig. 15c). The seismic moment of first sub-event is equal to an M_w 6.9 shock as revealed by seismological data (Antolik *et al*., 2004). Eastward rupture passed through the Sun Lake, and then jumped onto the main trace of the Kusai Lake fault at 91º07'E in the southeast of the Buka Daban Peak (Figs. 7a and 15c). The second sub-event occurred near 92º15'E, which is similar with location of Harvard Moment Centriod (Bufe, 2004). The second sub-event is a major rupture event, which is equal to an M_w 7.8 event (Antolik *et al*., 2004). The rupture from the second sub-event continuously propagated eastward and passed through the Kusai Lake and south slope of the Kunlun Range. It triggered the third sub-event near 93º00'E (Fig. 15c), which is the same with the location of third sub-event suggested by Xu and Chen (2004). The seismic moment of third sub-event is equal to an M_w 6.7 event (Antolik *et al*., 2004). Then, it continuously propagated eastward along the Kunlun Pass fault, but the fracture energy gradually dropped. Finally, it terminated near 94º58'E (Fig. 15c). Temporally, the second and third sub-events occurred 52 and 56 seconds, respectively, after the first sub-event as revealed by seismological data (Xu and Chen, 2004). However, our model is different from the unilateral rupture process inferred from the inversion of seismic data (Lin *et al.*, 2003; Antolik *et al.*, 2004). Our model suggests that rupture caused by the second sub-event also propagated westward. At the east of the Buka Daban Peak, the rupture propagated southwestward, and terminated near 91º07'E (Figs. 3b and 15c). It can reasonably explain the complex geometry pattern of surface rupture zone in the southeast of the Buka Daban peak (Fig. 7). It should be noted that a 30 km long rupture gap exists between the Sun Lake and Buka Daban-Hongshui River segments (Fig. 3b). It probably is an unbroken barrier (Aki, 1984).

5.2 Length of the surface rupture

It remains a debate about the length of the 2001 Kunlun surface rupture zone. For example, Xu *et al.* (2002) reported a ~350 km long rupture zone extending between 91º07'E-94º48'E. The high-precision mapping of satellite images clearly indicate that the five first-order rupture segments are 65 km, 110 km, 55 km, 70 km and 130 km for the Sun Lake, Buka Daban-Hongshui River, Kusai Lake, Hubei Peak and Kunlun Pass segments, respectively (Figs. 3b, 6b, 9b and 13b). Thus, the total length of the surface rupture zone should be ~430 km (excluding a 30 km long gap). This spatial distribution of surface rupture zone has also been confirmed by the field observations (Figs. 5b, 10b and 14b; Zhao *et al.*, 2002; Fu *et al.*, 2004a), and it is also consistent with the distribution of aftershocks (Fig. 15a). The previous reported longest surface rupture zone is 375 km long, which was produced by 1905 M 8.2 Bulnay, Mongolia, earthquake (Yeats *et al.*, 1997). The surface rupture zone produced by the 2001 M_w 7.8 Kunlun earthquake is, therefore, the longest rupture zone produced by a single intraplate earthquake ever reported worldwide.

5.3 Implications for future earthquakes along the Kunlun fault

The previous studies have demonstrated that the segment boundaries linking the fault segments are unstable features and earthquake can easily occur near the segment boundary (e.g., King and Nabelek, 1985; Fu *et al.*, 2004b). Therefore, it should be noted that the 2001 Kunlun earthquake did not rupture the Xidatan-Dongdatan segment of the Kunlun fault system (Figs. 13b and 15a). It is a "seismic gap" between the 1937 M_s 7.5 Tuosuo Lake earthquake and the 2001 M_w 7.8 Kunlun earthquake (Fig. 1b). Tectono-geomorphic feature shows that it is a large pull-apart basin, in which a large earthquake event may occur in the future. In the Xidatan area, engineering design of the Qinghai-Tibet railway under construction thus should consider the future possible large earthquake. The special engineering design of the Trans-Alaska oil pipeline, which did not break during the 2002 M_w 7.9 Denali Fault earthquake, provides a successful example (Phillips *et al.*, 2003).

6. Conclusions

Based on the detailed analyses of satellite images and field observations, we can conclude as follows:

(1) The 2001 November surface rupture zone can be divided into five first-order segments according to the geometry of surface rupture zone. These first-order segments, each 55 to 130 km long, are linked by large step-overs and bends. These first-order segments are further divided into over 20 second-order segments, each 10 to 30 km long, by smaller step-overs and bends.

(2) Rupture propagation process associated with the 2001 Kunlun earthquake is quite complex. It suggested that multi-segment geometry of the 2001 Kunlun rupture zone is a product of the multiple westward and eastward rupture propagation, and interaction of these bilateral rupture propagation, which is consistent with rupture process of three major sub-events suggested by seismological research.

(3) High precision measurement shows that total length of surface rupture zone is ~430 km, which is the longest one among the intraplate earthquakes ever reported worldwide.

In general, the analyses of the 2001 surface rupture zone provide new insights into the complex multi-segment geometry and multiple bilateral rupture propagation associated with a great intraplate earthquake along a long strike-slip fault.

Acknowledgements

This study benefited from discussion with A. Lin, K. Kano, E. Tsukuda, Y. Sugiyama, X. Lei, M. Saito and H. Sekiguchi. We thank K. Satake for his constructive comments and careful review, which are helpful to improve this manuscript. ASTER data were provided by the Earth Remote Sensing Data Analysis Center (ERSDAC), Japan. We also used the DEM data released by USGS Shuttle Radar Topography Mission (SRTM) Project in Fig. 1a. Especially, we are grateful to Seismological Bureau of Xinjiang for the permission to use one photograph (Fig. 5b). B. Fu would like to acknowledge the support from Postdoctoral Fellowship (P 03510) of Japan Society for the Promotion of Science (JSPS).

References

Aki, K. (1984) Asperities, barriers, characteristic earthquakes and strong motion prediction. *J. Geophys. Res.*, **89**, 5867-5872.

Allen, C.R. (1968) The tectonic environments of seismically active and inactive areas along the San Andreas fault system. In: Dickinson, W.R., and Grantz, A. (Eds.), Conference on Geologic Problems of San Andreas Fault System, Stanford University Publication in Geological Sciences, **11**, 70-80.

Allen, C. R., Luo. Z., Qian, H., Wen, X., Zhou, H., and Huang, W. (1991) Field study of a highly active fault zone: The Xianshuihe fault of southwestern China.

Geol. Soc. Am. Bull., **103**, 1178-1199.
Ambraseys, N.N. (1970) Some characteristic features of the Anatolian fault zone. *Tectonophysics*, **9**, 143-165.
Antolik, M., Abercrombie, R.E., and Ekstrom, G. (2004) The 14 November 2001 Kokoxili (Kunlunshan), Tibet, earthquake: Rupture transfer through a large extensional step-over. *Bull. Seismol. Soc. Am.*, **94**, 1173-1194.
Avouac, J.P., Tapponnier, P. (1993) Kinematic model of active deformation in central Asia. *Geophys. Res. Lett.*, **20,** 895-898.
Awata, Y., Yoshioka, T., Tsukuda, E., Emre, O., Duman, T.Y., and Dogan, A. (2001) Segment structure of the surface ruptures associated with the 1999 Izmit earthquake, North Anatolian fault system, Turkey. *Ann. Report on Active Fault and Paleoearthq. Res.,* **1**, 325-338 (in Japanese with English abstract).
Aydin, A., and Kalafat, D. (2002) Surface ruptures of the 17 August and 12 November 1999 Izmit and Duzce earthquakes in northwestern Anatolia, Turkey: Their tectonic and kinematic significance and the associated damage. *Bull. Seismol. Soc. Am.*, **92**, 95-106.
Barka, A.A., and Kadinsky-Cade, K. (1988) Strike-slip fault geometry in Turkey and its influence on earthquake activity. *Tectonics*, **7**, 663-684.
Bufe, C.G. (2004) Comparing the November 2002 Denali and November 2001 Kunlun earthquakes. *Bull. Seismol. Soc. Am.*, **94**, 1159-1165.
China Seismological Bureau (CSB) (2002) The 2001 M_s 8.1 West Kunlun Pass earthquake, China. Seismological Press, Beijing, 129 p. (in Chinese).
China Seismological Bureau (CSB) (2003) Album of the Kunlun Pass West M_s 8.1 earthquake, China. Seismological Press, Beijing, 105 p. (in Chinese with English abstract).
Dang, G., and Wang, Z. (2002) Characteristics of the surface rupture zone and main seismic hazards caused by the M_s 8.1 earthquake west of the Kunlun Pass, China. *Geol. Bull. China*, **21**, 105-108. (in Chinese with English abstract).
DePolo, C.M., Clark, D.G., Slemmons, D.B., and Ramelli, A.R. (1991) Historical surface faulting in the Basin and Range Province, western North America: implications for fault segmentation. *J. Struct. Geol.*, **13**, 123-136.
Dooley, T., and McClay, K. (1997) Analog modeling of pull-apart basins. *AAPG Bull.*, **81**, 1804-1826.
Fu, B., and Lin, A. (2003) Spatial distribution of the surface rupture zone associated with the 2001 M_s 8.1 Central Kunlun earthquake, northern Tibet, revealed by satellite remote sensing data. *Int. J. Remote Sens.*, **24**, 2191-2198.
Fu, B., Awata, Y., Kano, K., Lin, A., Tsukuda, E. (2003) Coseimsic surface deformation and engineering damage associated with the large strike-slip faulting: Lessons from the 2001 M_w 7.8 Central Kunlun earthquake. *Ann. Report on Active Fault and Paleoearthq. Res.,* **3**, 191-209.
Fu, B, and Awata, Y. (2004) When the Kunlun Fault began its left-lateral strike-slip faulting: Evidence from cumulative offset of basement rocks and geomorphic features. *Himalayan Journal of Sciences*, **2**, 132.
Fu, B., Awata, Y., Du, J., and He, W. (2004a) Surface deformations associated with the 2001 M_w 7.8 Kunlun earthquake, northern Tibet: geomorphic growth features along a major strike-slip fault. *Engineering Geology*, **75**, 325-339.
Fu. B., Ninomiya, Y., Lei, X., Toda, S., and Awata, Y. (2004b) Mapping the active strike-slip fault triggered the 2003 M_w 6.6 Bam, Iran, earthquake with ASTER 3D images. *Remote Sens. Environ.,* **92**, 153-157.
Jia Y., Dai, H., Su, X. (1988) Tuosuo Lake earthquake fault in Qinghai Province. In: Xinjiang Seismological Bureau (Eds.), Research on Earthquake Faults in China. Xinjiang People`s Press, Urumqi, pp.66-71. (in Chinese).
Kidd, W.S.F., Molnar, P. (1988) Quaternary and active faulting observed on the 1985 Academia Sinica-Royal Society geotranverse of Tibet. *Phil. Trans. R. Soc. Lon.*, **327**, 337-363.
King, G.C.P (1986) Speculations on the geometry of initiation and termination processes of earthquake rupture and its relation to morphology and geological structures. *Pure and Applied Geophysics*, **124**, 567-585.
King, G.C.P., and Nabelek, J. (1985) Role of fault bends in the initiation and termination of earthquake rupture. *Science*, **228**, 984-987.
Lin, A., Fu, B., Guo, J., Zeng, Q., Dang, G., He, W., and Zhao, Y. (2002) Co-seismic strike-slip and rupture length produced by the 2001 M_s 8.1 Central Kunlun earthquake. *Science*, **296**, 2015-2017.
Lin, A., Kikuchi, M., and Fu, B. (2003) Rupture segmentation and process of the 2001 M_w 7.8 Central Kunlun, China, earthquake. *Bull. Seismol. Soc. Am.*, **93**, 2477-2492.
McClay, K., and Bonora, M. (2001) Analog models of restraining stopovers in strike-slip fault systems. *AAPG Bull.*, **85**, 233-260.
Molnar, P., and Tapponnier, P. (1975) Cenozoic tectonics of Asia: Effects of continental collision. *Science,* **189**, 419-426.
Molnar, P., and Tapponnier, P. (1978) Active tectonics of Tibet. *J. Geophys. Res.*, **83**, 5361-5375.
Phillips, D.E., Haeussler, P.J., Freymueller, J.T., and other 26 authors (2003) The 2002 Denali fault earthquake, Alaska: A large magnitude, slip-partitioned event. *Science*, **300**, 1113-1118.
Peltzer, G., Tapponnier, P., and Armijo, R. (1989) Magnitude of late Quaternary left-lateral displacements along the north edge of Tibet. *Science*, **246**, 1285-1289.
Peltzer, G., Grampe, F., King, G. (1999) Evidence of nonlinear elasticity of the crust from the M_w 7.6 Manyi earthquake. *Science,* **286,** 272-276.
Schultz, R.A. (1999) Understanding the process of

faulting: selected challenges and opportunities at the edge of the 21st century. *J. Struct. Geol.*, **21**, 985-993.

Schwartz, D.P., and Sibson, R.H. (1989) Fault segmentation and controls of rupture initiation and termination. U.S. Geological Survey Open File Report **89-315**, 447p.

Schwartz, D.P., and Coppersmith, K.J. (1984) Fault behavior and characteristic earthquakes: examples from the Wasatch and San Andreas fault zones. *J. Geophys. Res.*, **89**, 5681-5698.

Segall, P., and Pollard, D.D. (1980) Mechanics of discontinuous faults. *J. Geophys. Res.*, **85**, 4337-4350.

Seismological Bureau of Qinghai Province and the Institute of Crustal Dynamics, China Seismological Bureau (SBQP) (1999) Eastern Kunlun Active Fault Zone. Seismological Press, Beijing, 186 p. (in Chinese with English abstract).

Stein, R.S., Barka, A.A., and Dietrich, H.J. (1997) Progressive failure on the North Anatolian fault since 1939 by earthquake stress triggering. *Geophys. J. Int.*, **128**, 594-604.

Sugiyama, Y., Sekiguchi, H., and Awata, Y. (2002) Correlation analysis between active fault parameters and heterogeneous source characteristics. In: Study on the Master Model for Strong Ground Motion Prediction toward Earthquake Disaster Mitigation, pp.37-42 (in Japanese with English abstract).

Tapponnier, P., Xu, Z., Roger, F., Meyer, B., Arnaud, N., Wittlinger, Yang, J. (2001) Oblique stepwise rise and growth of the Tibet Plateau. *Science*, **294**, 1671-1677.

Van der Woerd, J., Ryerson, F. J., Tapponnier, P., Gaudemer, Y., Finkel, R.C., Meriaux, A.S., Caffee, M. W., Zhao, G., and He, Q. (1998) Holocene left slip-rate determined by cosmogenic surface dating on the Xidatan segment of the Kunlun Fault (Qinghai, China). *Geology*, **26**, 695-698.

Van der Woerd, J., Ryerson, F. J., Tapponnier, P., Meriaux, A.S., Gaudemer, Y., Meyer, B., Finkel, R.C., Caffee, M. W., Zhao, G., and Xu, Z. (2000) Uniform slip-rate along the Kunlun Fault: Implications for seismic behavior and large-scale tectonics. *Geophys. Res. Lett.*, **27**, 2353-2356.

Van der Woerd, J., Tapponnier, P., Ryerson, F. J., Meriaux, A.S., Meyer, B., Gaudemer, Y., Finkel, R.C., Caffee, M. W., Zhao, G., and Xu, Z. (2002) Uniform postglacial slip- rate along the central 600 km of the Kunlun fault (Tibet), from ^{26}Al, ^{10}Be, and ^{14}C dating of riser offsets, and climatic origin of the regional morphology. *Geophys. J. Int.*, **148**, 356-388.

Wallace, R.E. (1970) Earthquake recurrence intervals on the San Andreas fault. *Bull. Seismol. Soc. Am.*, **81**, 2875-2890.

Wallace, R.E. (1990) Geomorphic expression. In: Wallace, R.E. (Eds.), The San Andreas Fault System, California, U.S. Geological Survey Professional Paper **1515**, pp.15-58.

Ward, S.N. (1997) Dogtails versus rainbows: synthetic earthquake rupture models as an aid in interpreting geological data. *Bull. Seismol. Soc. Am.*, **87**, 1422-1441.

Wright, T.J., Parsons, B.E., and Lu, Z. (2004) Toward mapping surface deformation in three dimensions using InSAR. *Geophys. Res. Lett.*, **31**, L01607.

Xu, L., and Chen, Y. (2004) Temporal and spatial rupture process of the great Kunlun earthquake of November 14, 2001 from the Gdsn long period waveform data. *Science in China (Ser.D)*, **34**, 256-264 (in Chinese).

Xu, X., Chen, W., Yu, G., Ma, W., Dai, H., Zhang, Z., Chen, Y., He, W., Wang, Z. and Dang, G. (2002) Characteristic features of the surface ruptures of the Huh Sai Hu (Kunlunshan) earthquake (M_s 8.1), northern Tibetan Plateau, China. *Seismology and Geology,* **24**, 1-13 (in Chinese with English abstract).

Yeats, R.S., Seih, K., and Allen, C.R. (1997) The geology of earthquakes. Oxford University Press, New York, 568 p.

Zhang, P., Mao, F., and Slemmons, D. B. (1999) Rupture termination and size of segment boundaries from historical earthquake ruptures in the Basin and Range Province. *Tectonophysics*, **308**, 37-52.

Zhao, G. (1996) Quaternary faulting in the north Qinghai-Tibet Plateau. *Earthquake Research in China*, **12**, 107-119 (in Chinese with English abstract).

Zhao, R., Li, J., Xiang, Z., Ge, M., and Luo, G. (2002) Expedition of the west segment of the surface rupture zone of the M_s = 8.1 earthquake in the west of Kunlun Pass. *Inland Earthquake*, **16**, 175-179 (in Chinese).

(Received 19 August 2004, Accepted 5 October 2004)

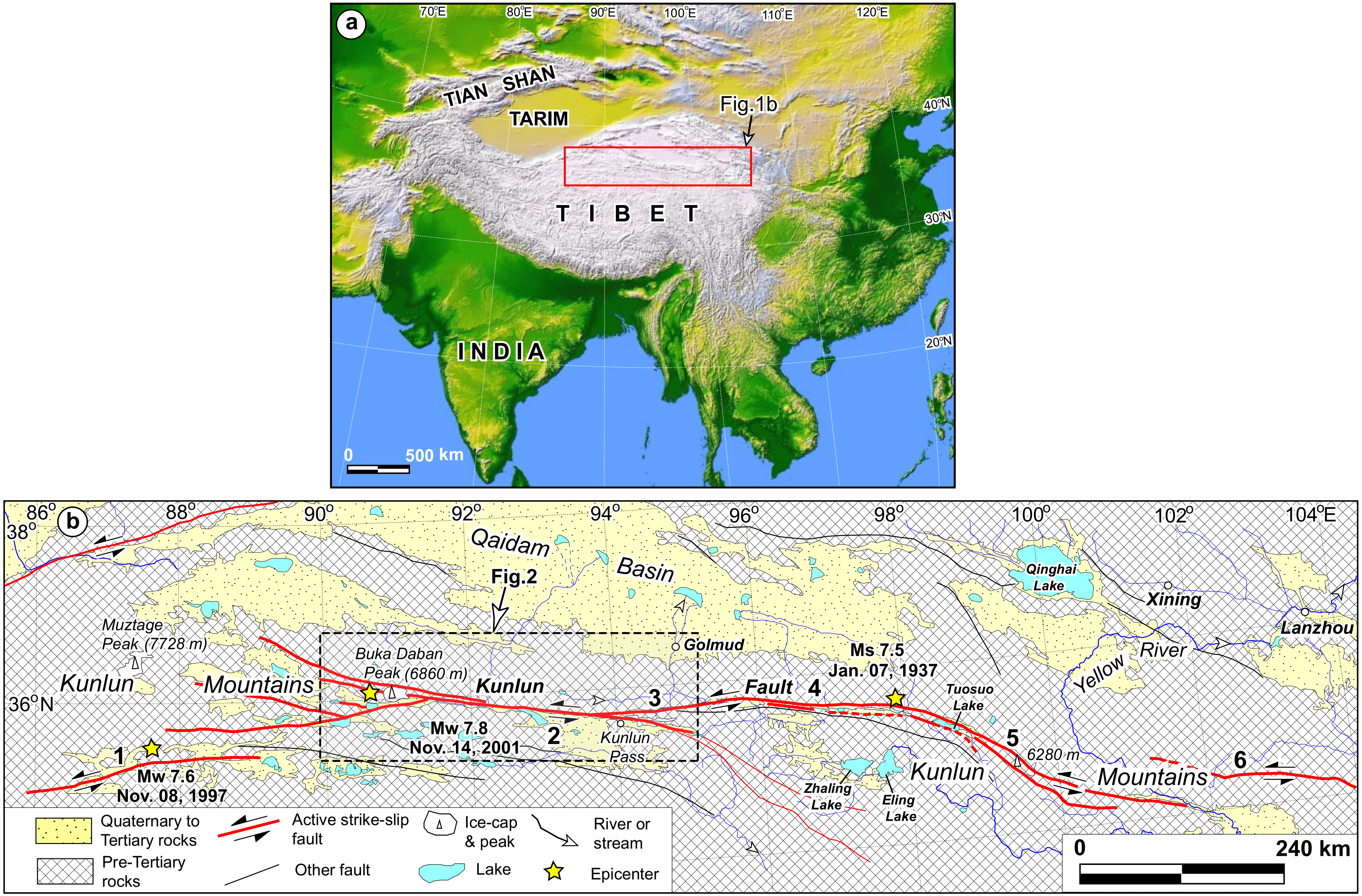

Fig. 1. (a) Shaded-relief image of the India-Asia collision zone, generated from the USGS Shuttle Radar Topography Mission DEMs. (b) Fault segmentation of the Kunlun fault system between 86° to 104° E. The numbers 1-6 represent the Manyi, Kusai Lake, Xidatan-Dongdatan, Tuosuo Lake, Maqen, and Min Shan faults, respectively. The epicenter of the 2001 Kunlun earthquake was determined by the U.S. Geological Survey (USGS).

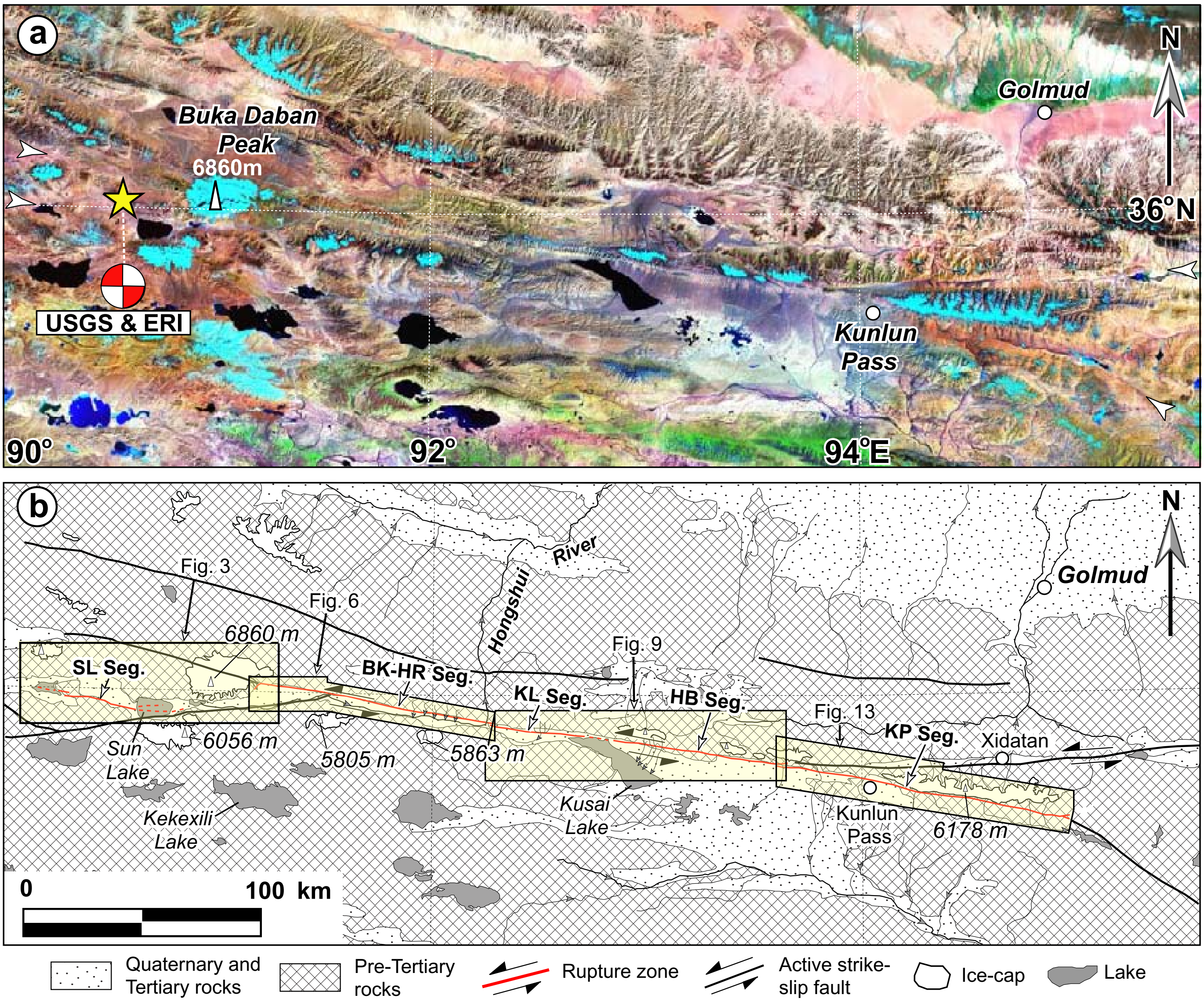

Fig. 2. (a) Landsat ETM mosaic image of the Kusai Lake and Kunlun Pass faults of the Kunlun fault system. Fault traces indicated by arrows. The epicenter and focal mechanism of the 2001 M_w 7.8 Kunlun earthquake were determined by the USGS and Earthquake Research Institute (ERI) of the University of Tokyo, respectively. (b) Spatial distribution of the surface rupture zone produced by the 2001 Kunlun earthquake (Modified after Fu and Lin, 2003). SL Seg.: Sun Lake segment; BK-HR Seg.: Buka Daban-Hongshui River segment; KL Seg.: Kusai Lake segment; HB Seg.: Hubei Peak segment; KP Seg.: Kunlun Pass segment.

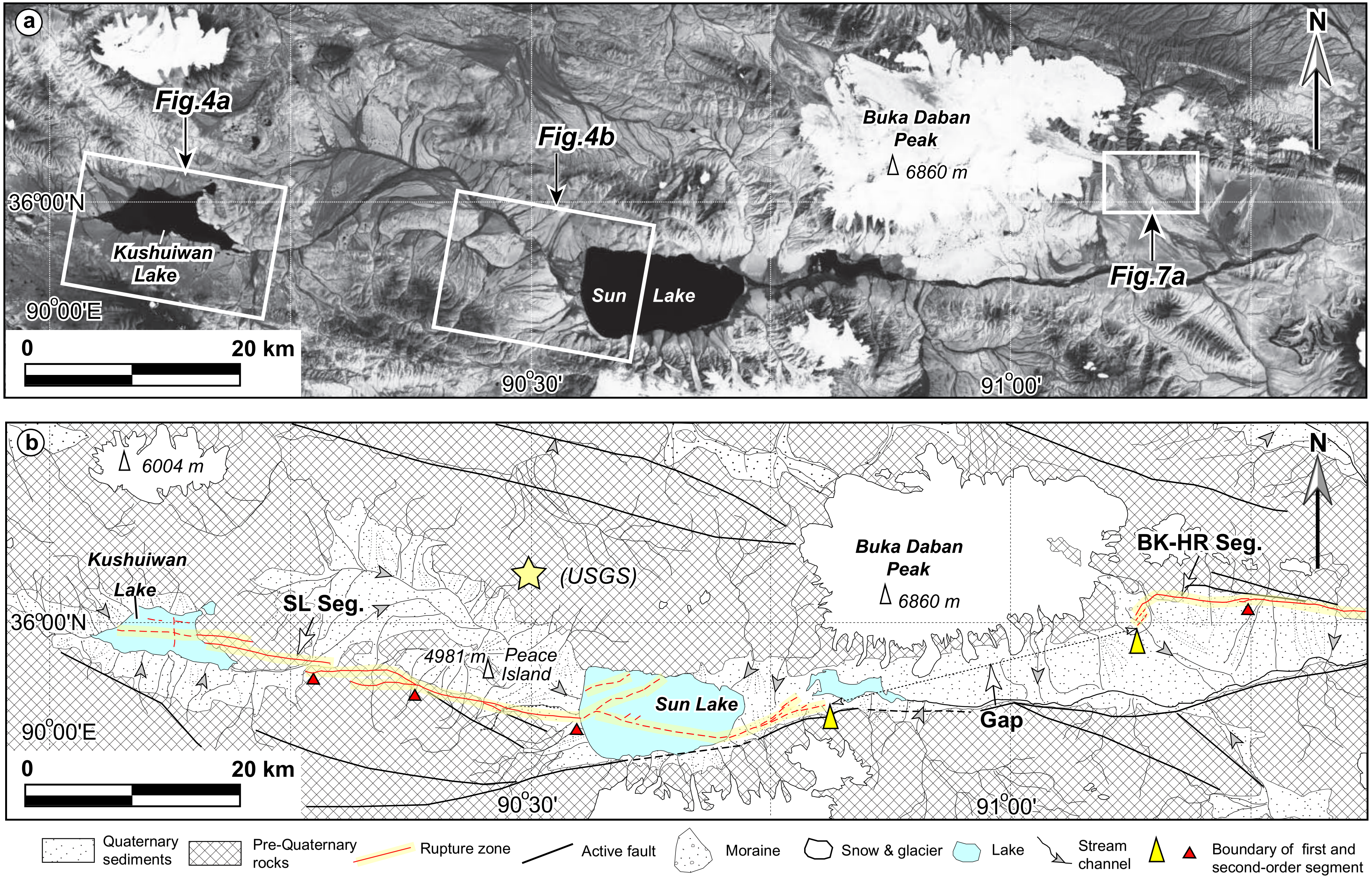

Fig. 3. (a) Landsat ETM image of the Sun Lake segment (August 16, 2002). (b) Interpretative map showing geometry of the west part of surface rupture zone. Note that there is a 30 km-long gap between 90°50'E and 91°07'E indicated by yellow triangles. For location see Fig. 2b.

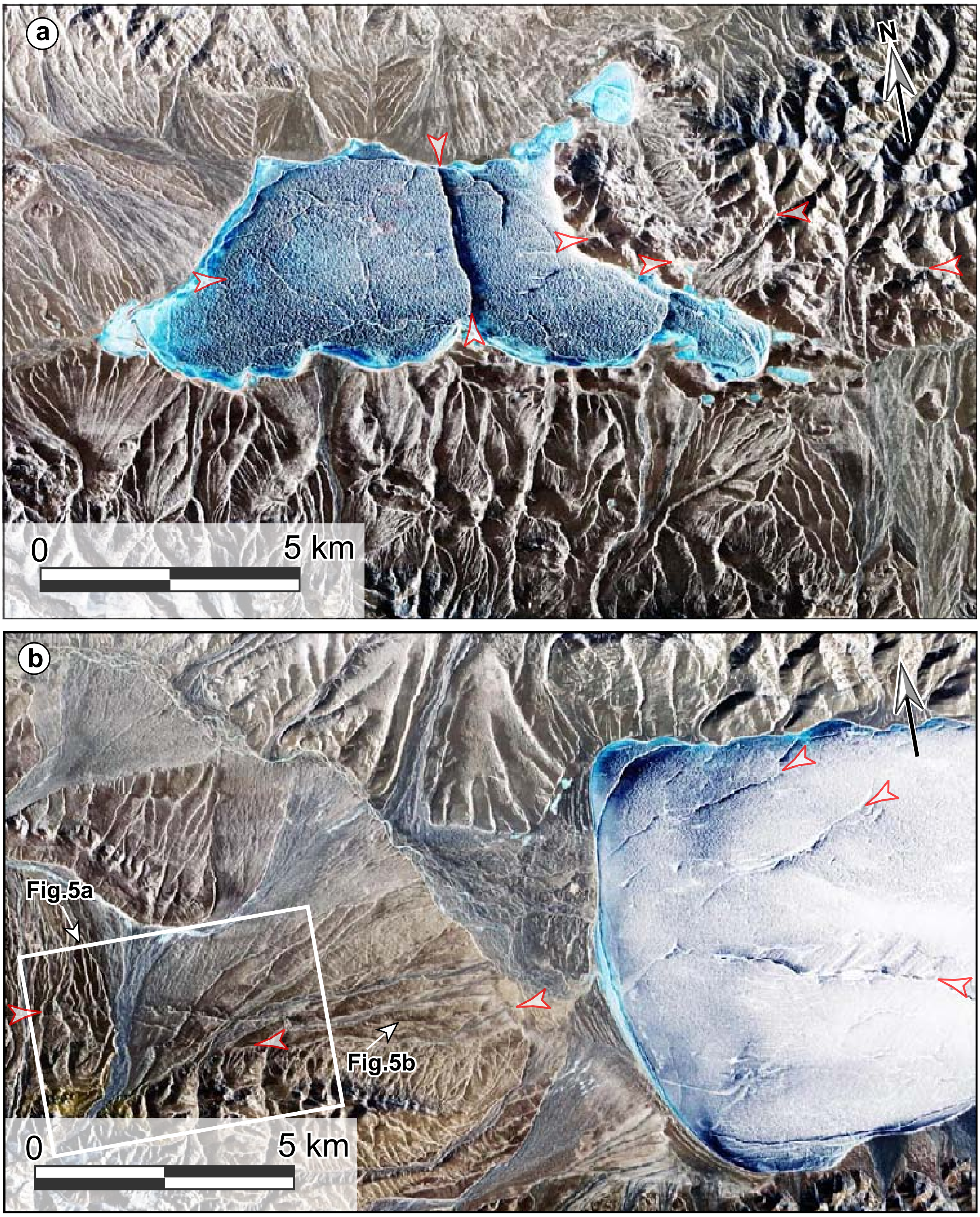

Fig. 4. Post earthquake (January 05, 2002) ASTER images exhibiting geometry of the surface rupture zone. (a) Ruptures appearing as right-stepping en-echelon pattern in the westernmost termination. (b) Ruptures displaying a tail pattern in the Sun Lake. Locations of Figs. 4a and 4b are shown on Fig. 3a.

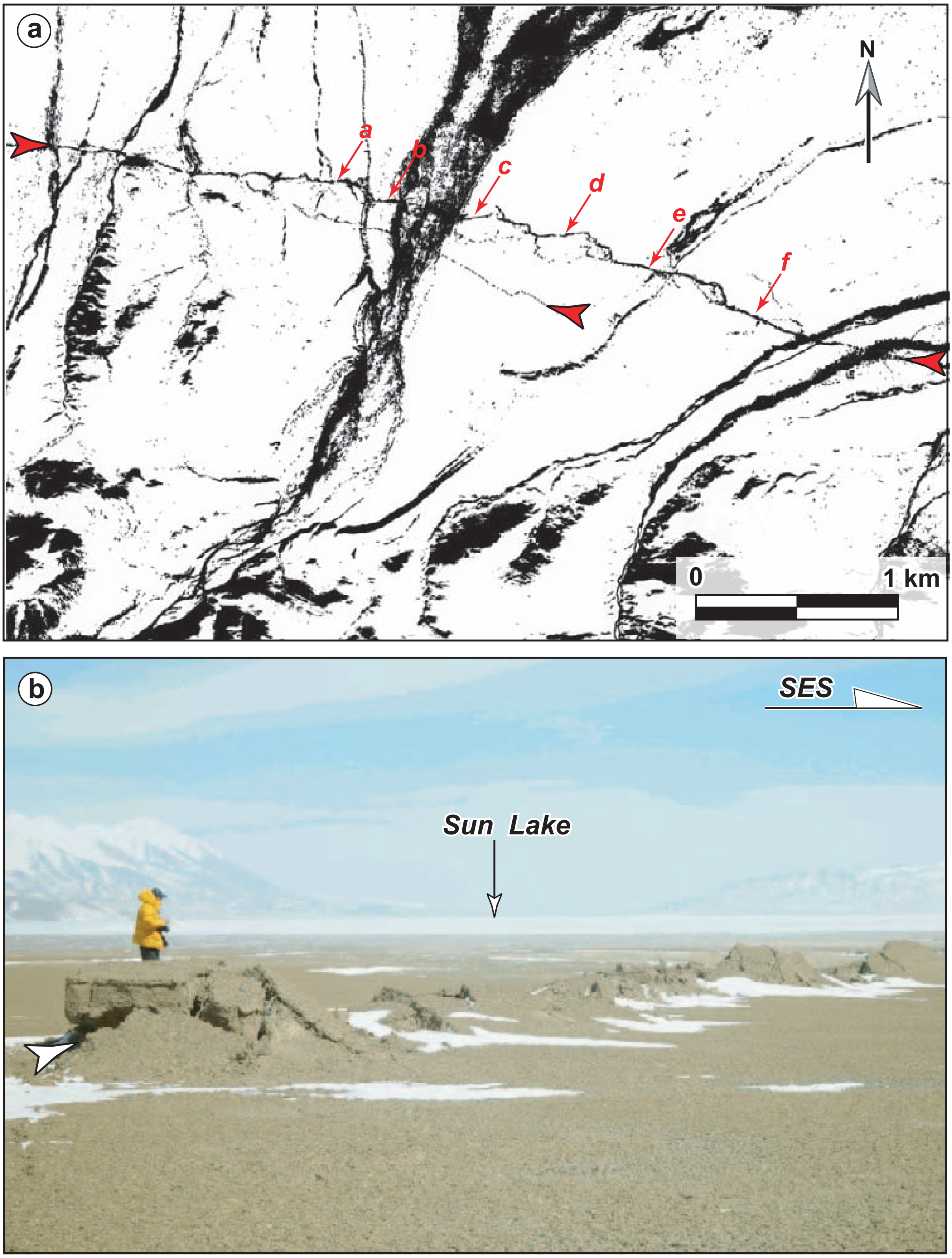

Fig. 5. (a) IKONOS image (September 24, 2002) showing detailed features of surface ruptures to west of the Sun Lake. For location see Fig. 4b. (b) Photograph showing a distinctive rupture in west bank of the Sun Lake (provided by Seismological Bureau of Xinjiang, CSB) .

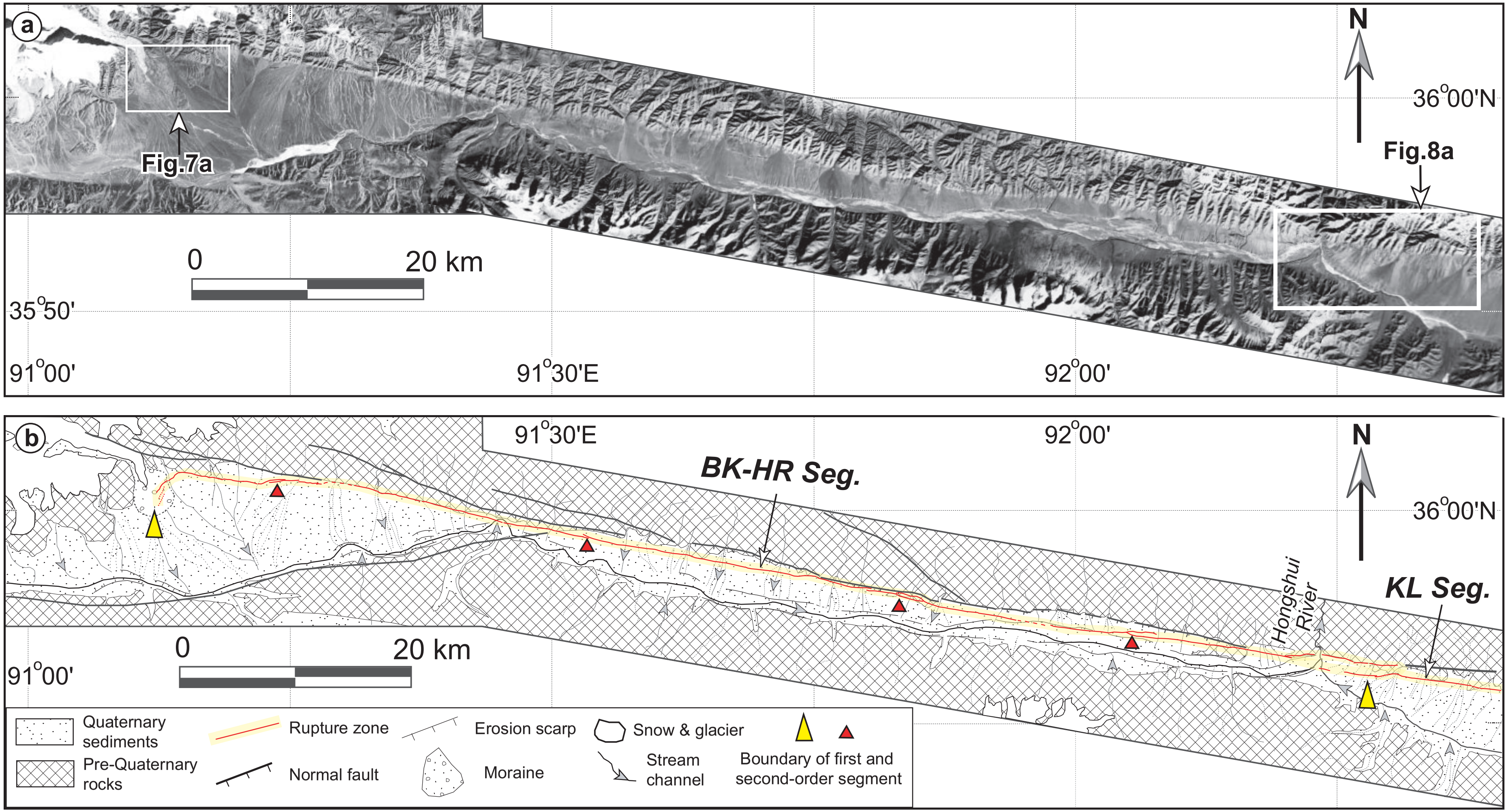

Fig. 6. (a) Satellite mosaic image showing geomorphic features of the Buka Daban-Hongshui River segment. (b) Interpretative map showing geometry of the Buka Daban-Hongshui River segment of the 2001 surface rupture zone. For location of Fig. 6 see Fig. 2b.

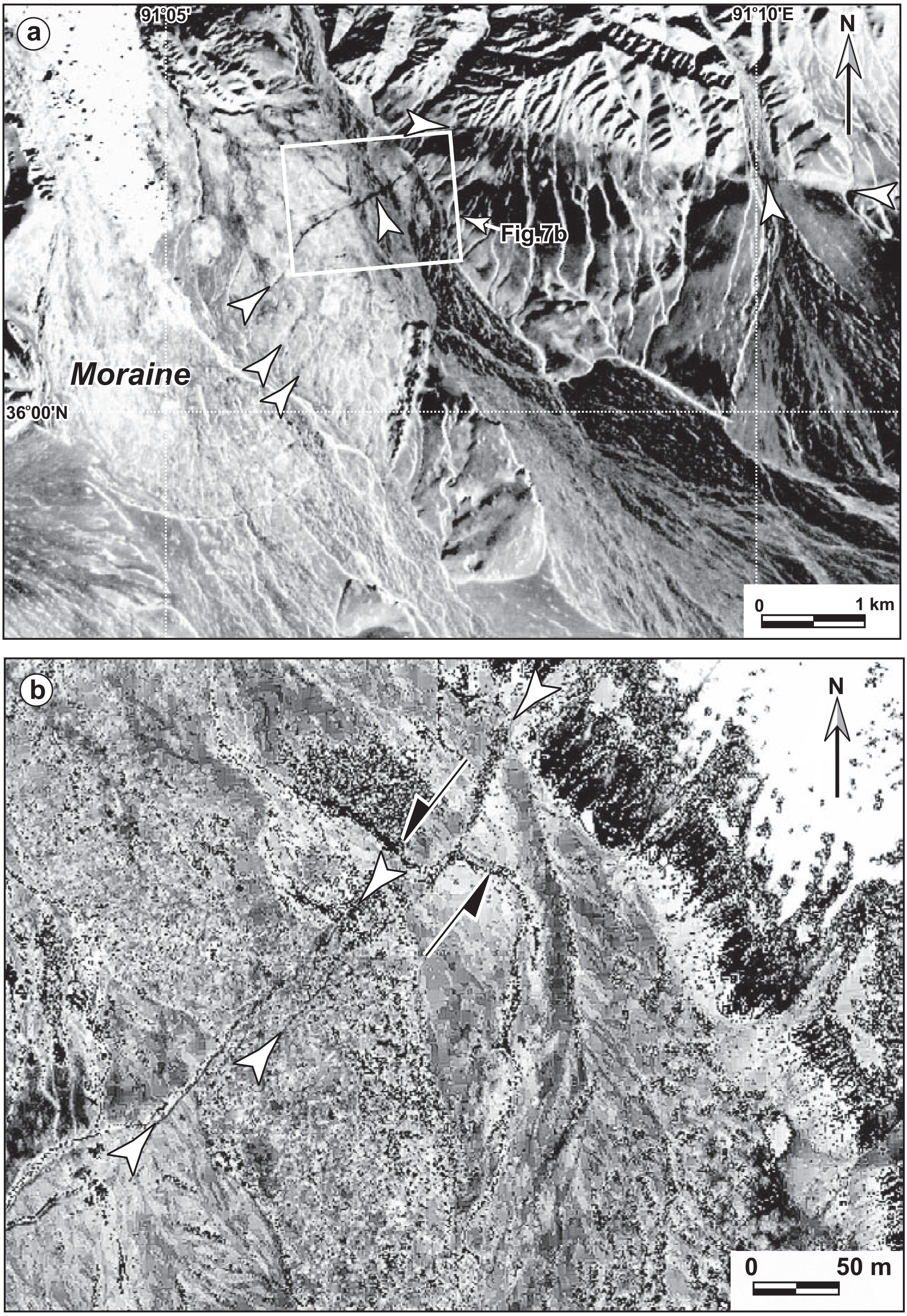

Fig. 7. (a) Post-earthquake (December 26, 2001) SPOT image showing tail pattern of surface rupture in the west end of Buka Daban-Hongshui River segment. For location see Fig. 3a or Fig. 6a. (b) IKONOS image (September 24, 2002) showing that the surface ruptures appear a right-stepping pattern in southeast of the Buka Daban Peak. For location see Fig. 7a.

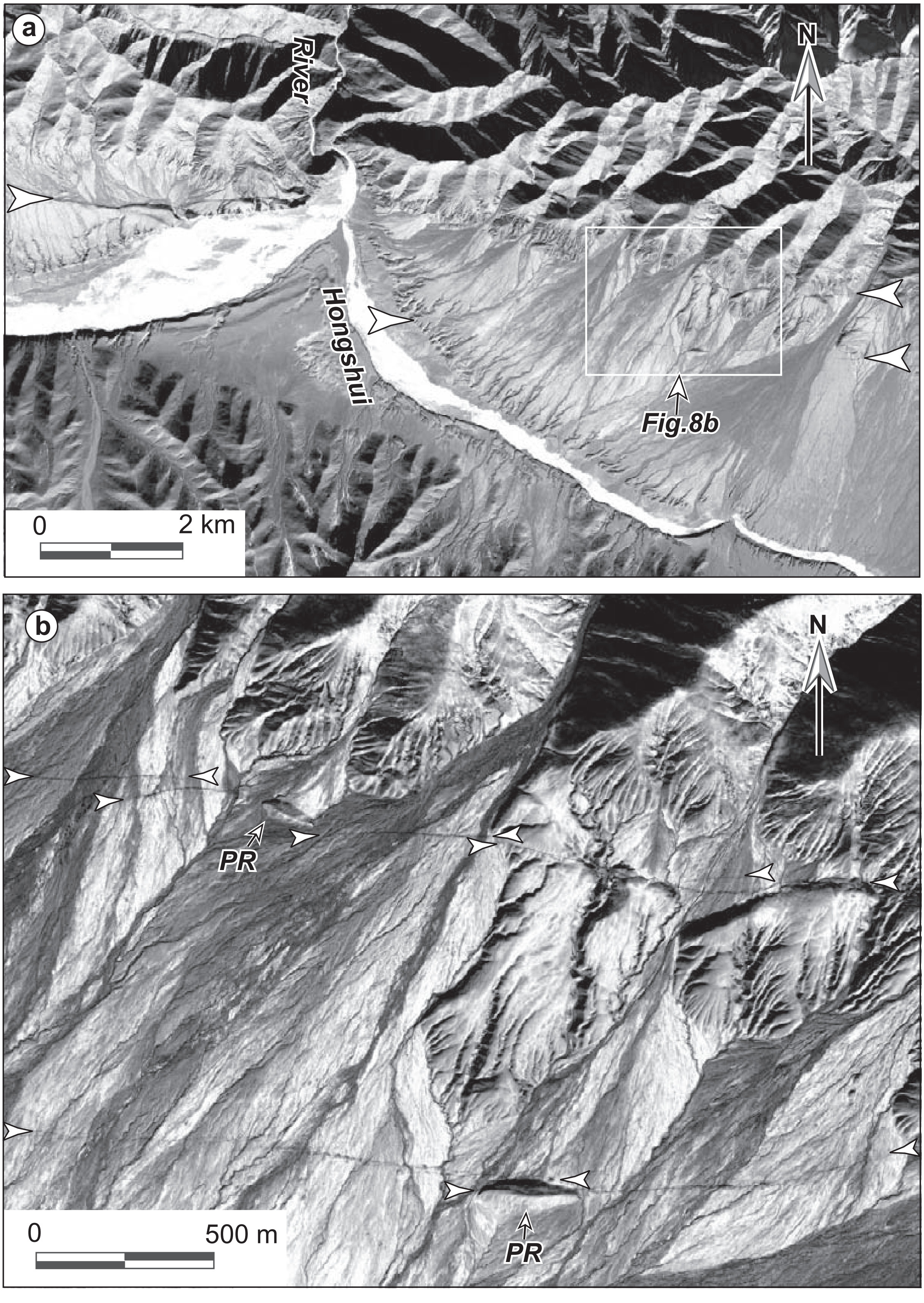

Fig. 8. (a) IKONOS image (January 9, 2002) showing that the segment boundary between the Buka Daban-Hongshui River and Kusai Lake segments appears as a step-over, 10 km long and 500 m wide. (b) Enlarged IKONOS image showing the detailed geometric and geomorphic features of the ruptures. Note that the ruptures are separated by third-order step-overs or bends. PR: pressure ridge.

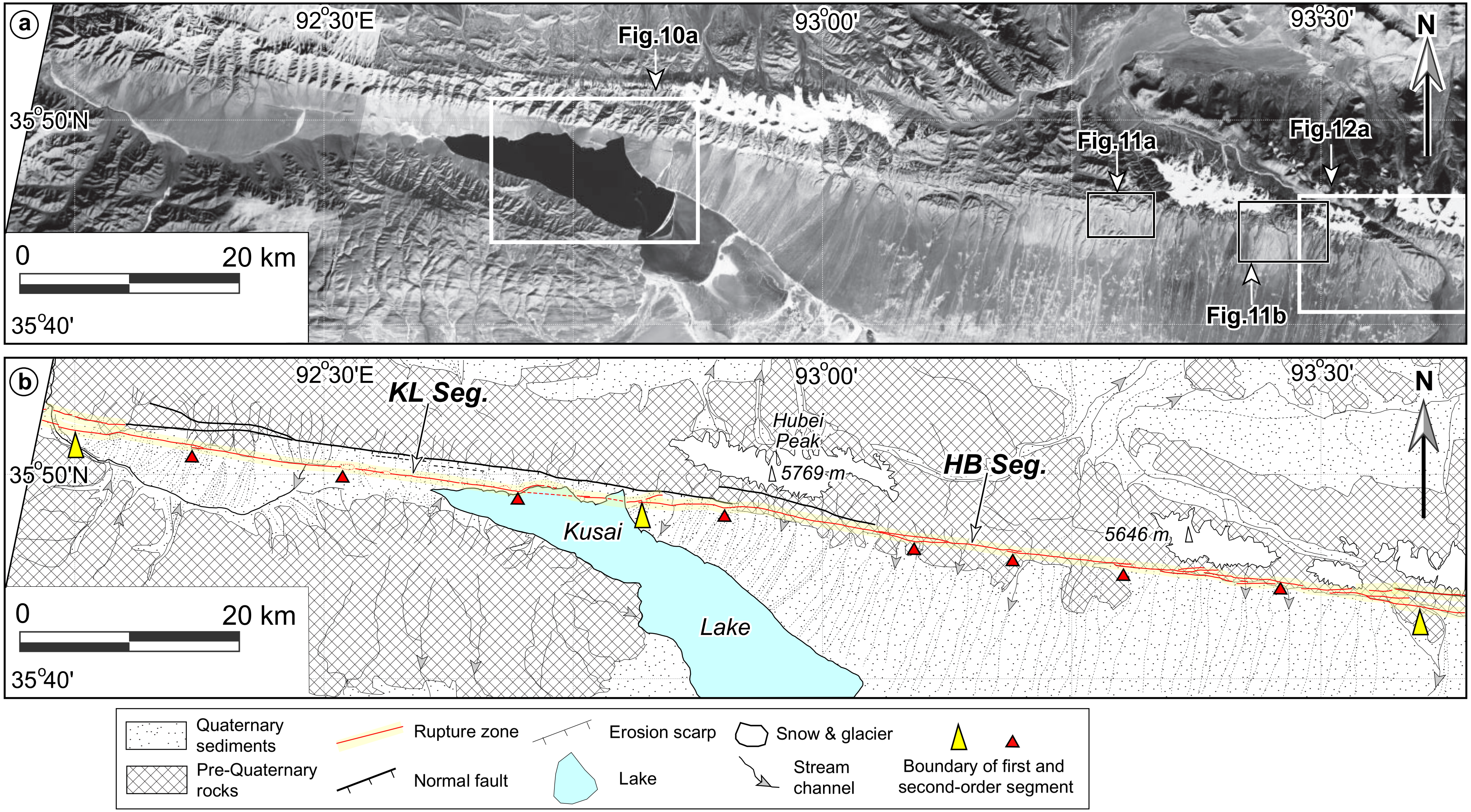

Fig. 9. (a) Satellite mosaic image showing geomorphic features of the Kusai Lake and Hubei Peak segments. (b) Interpretative map exhibiting geometry of the Kusai Lake and Hubei Peak segments of the 2001 coseismic surface rupture zone. For location see Fig. 2b.

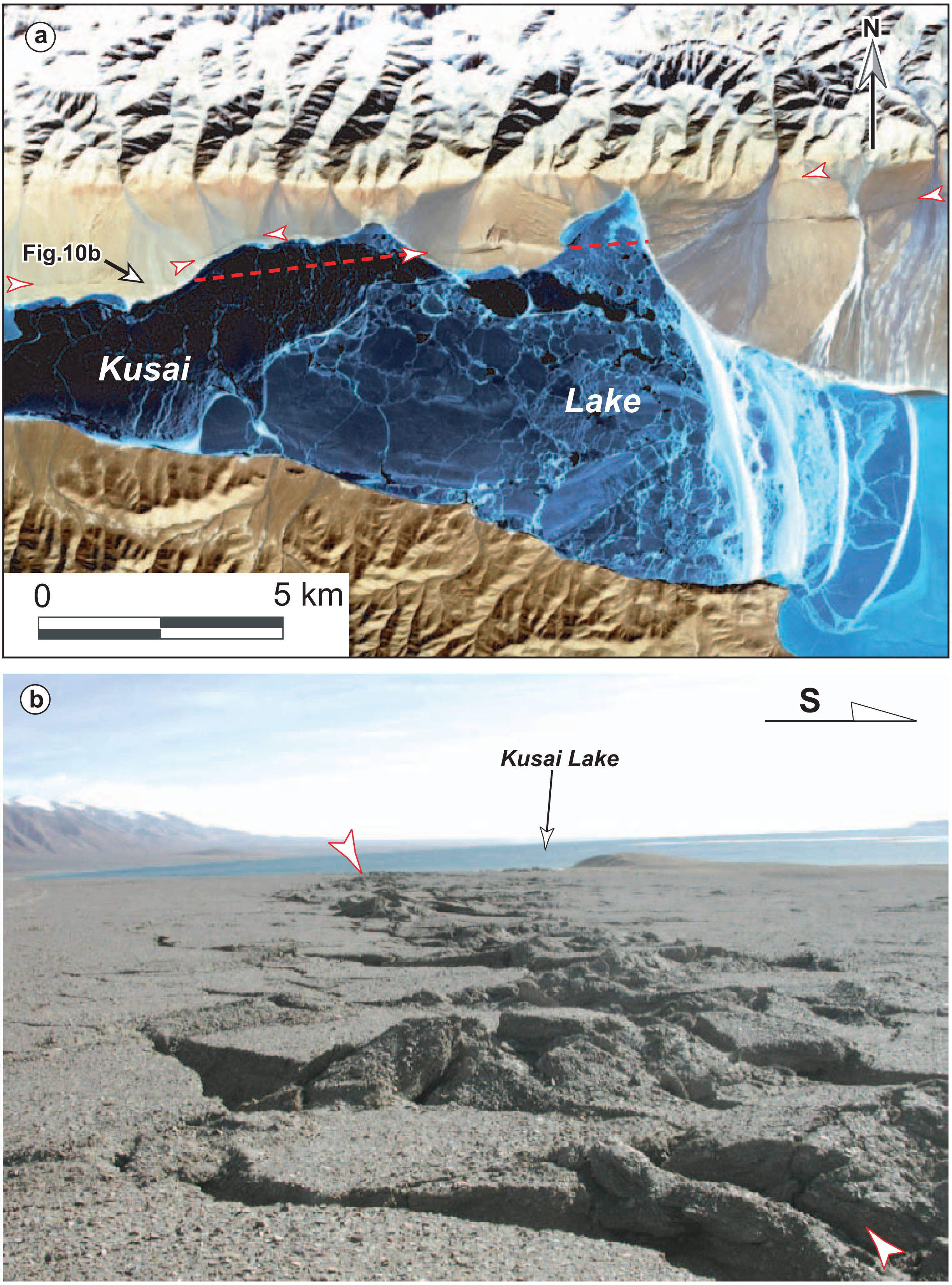

Fig. 10. (a) ASTER VNIR image (December 6, 2001) showing distinctive coseismic ruptures in the north of the Kusai Lake. For location see Fig. 9a. (b) Photograph showing the surface rupture zone in the northern bank of Kusai Lake. For location see Fig. 10a.

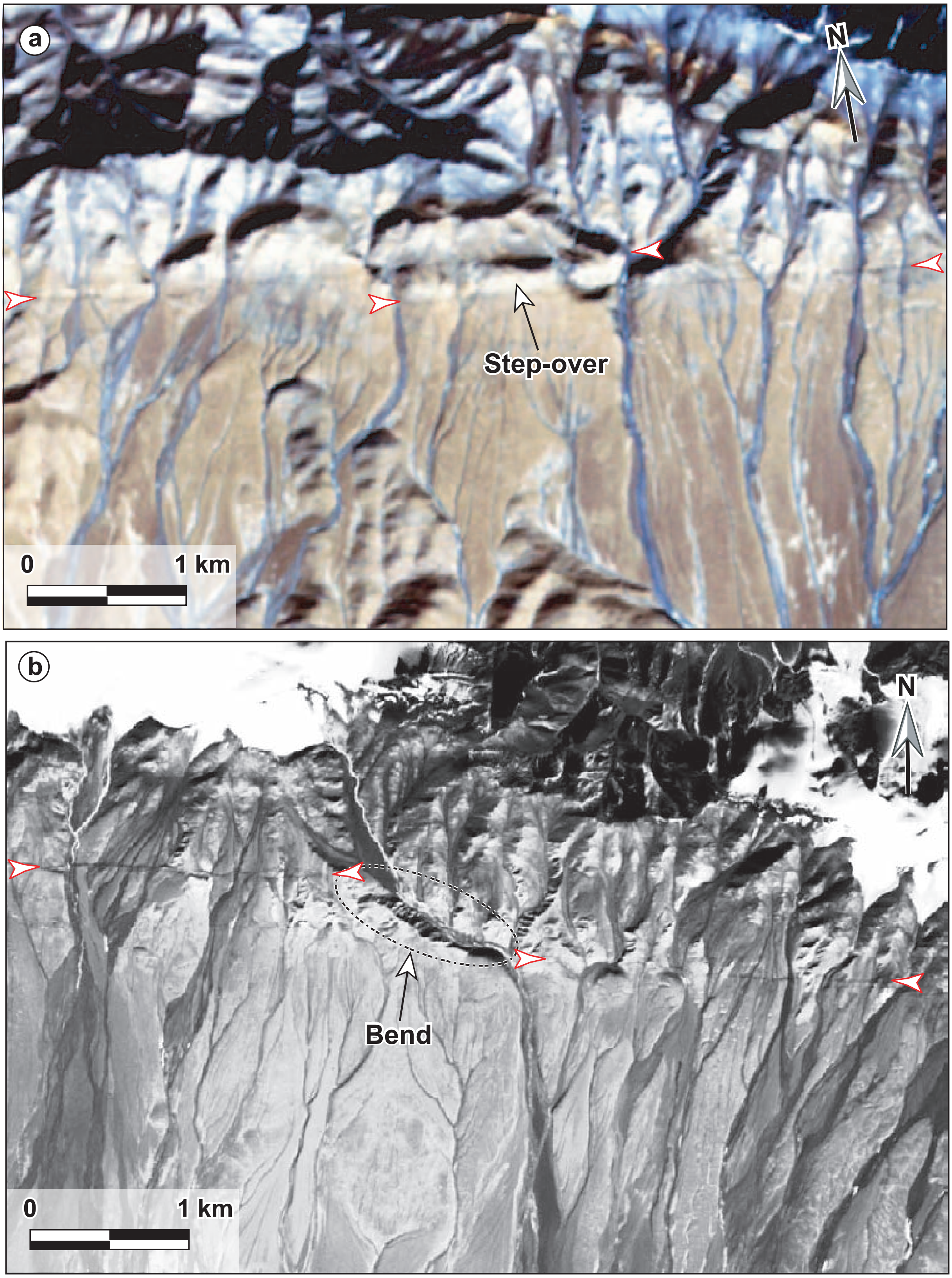

Fig. 11. (a) ASTER VNIR image (November 29, 2001) showing a right-stepping en-echelon pattern of the ruptures. Note that a pressure ridge formed between two ruptures in the northeast of the Kusai Lake. (b) SPOT image exhibiting a bend between two second-order segments in the Hubei Peak segment. For locations see Fig. 9a.

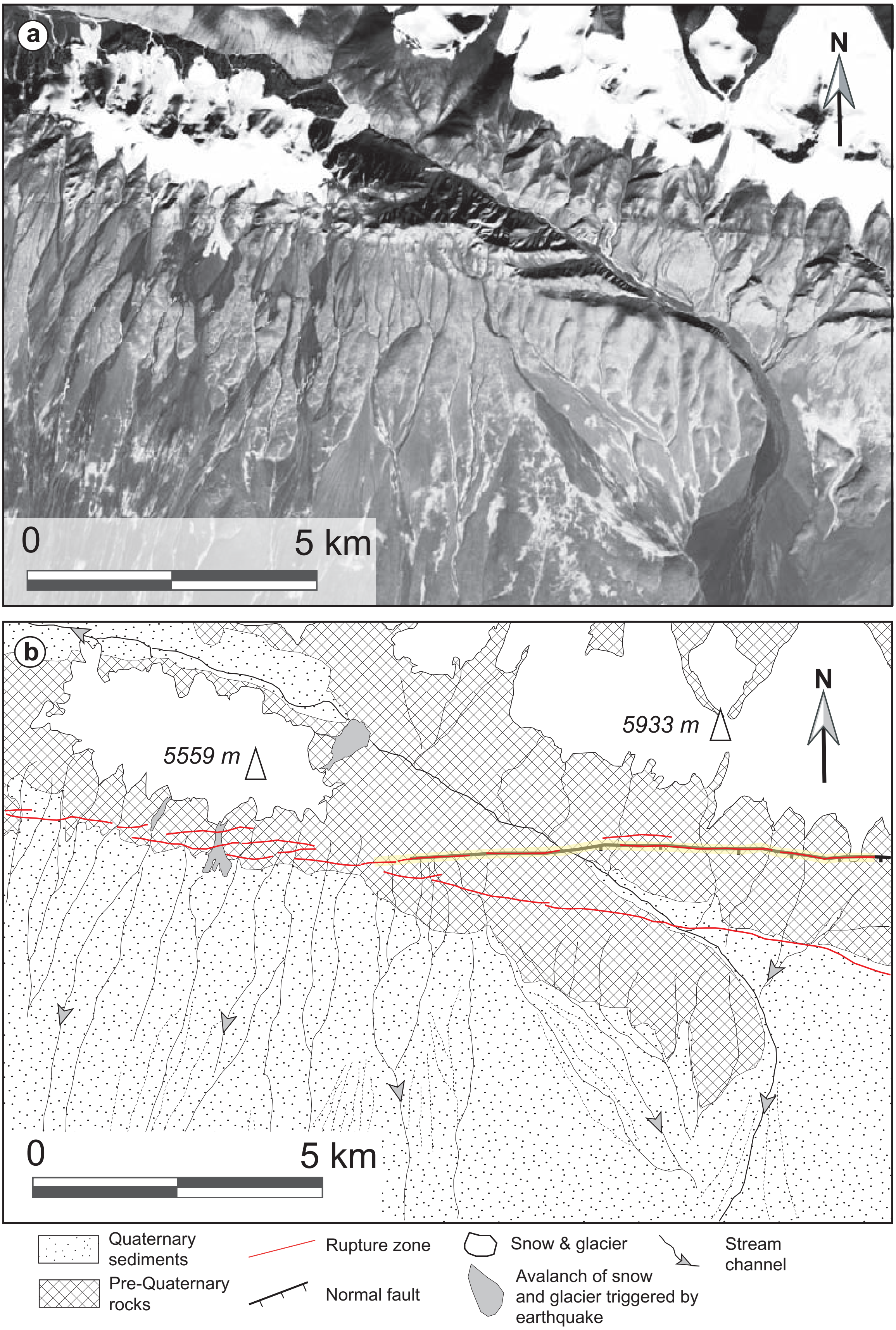

Fig. 12. (a) SPOT image (January 16, 2002) showing the segment boundary between the Hubei Peak and Kunlun Pass segments. The segment boundary appears as a step-over, where the ruptures display a complicated pattern. (b) Interpretative map displaying the step-over between two segments. For location see Fig. 9a.

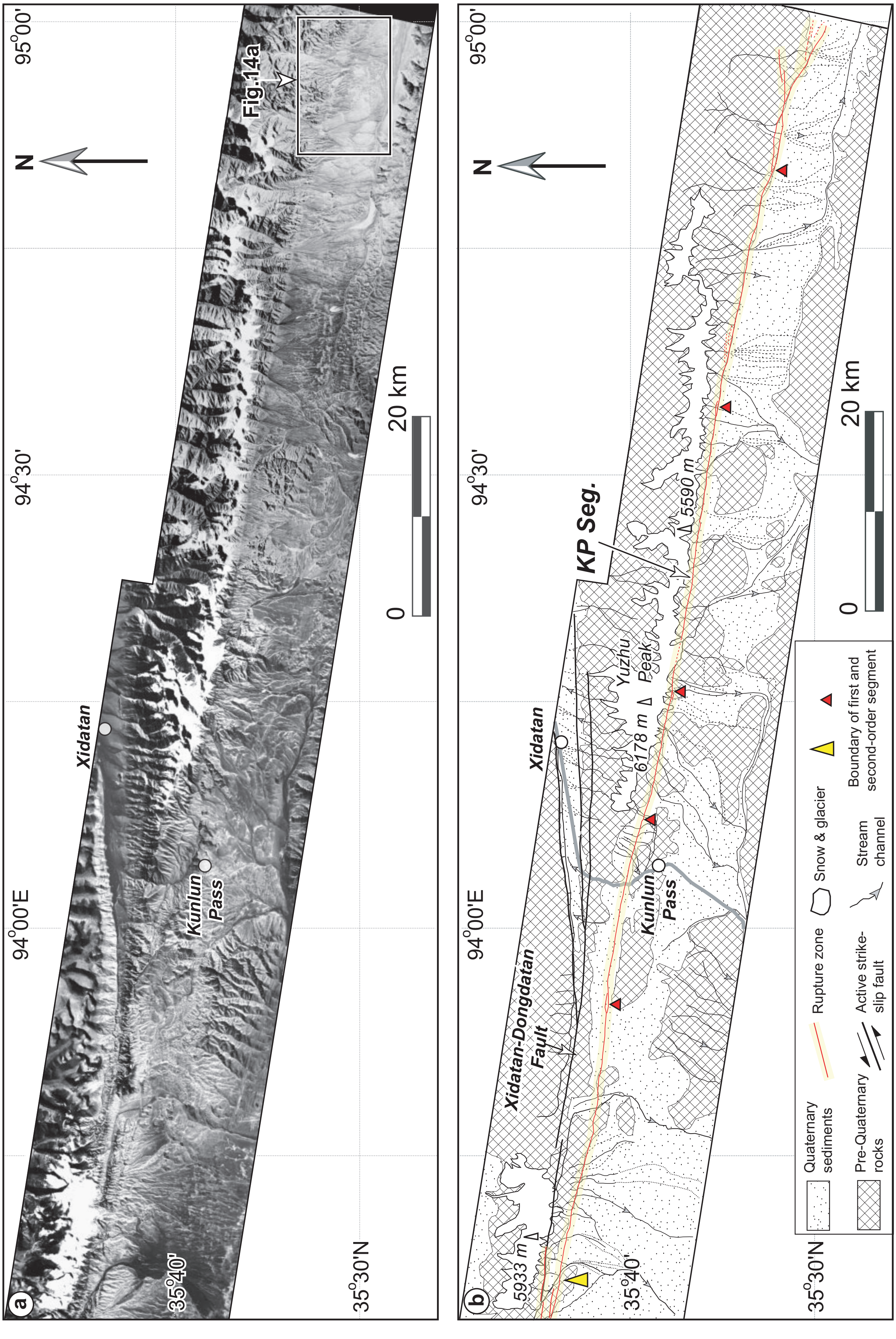

Fig. 13. (a) Satellite mosaic image exhibiting geomorphic features of the Kunlun Pass segment. (b) Interpretative map showing geometry of the Kunlun Pass segment. For location see Fig. 2b.

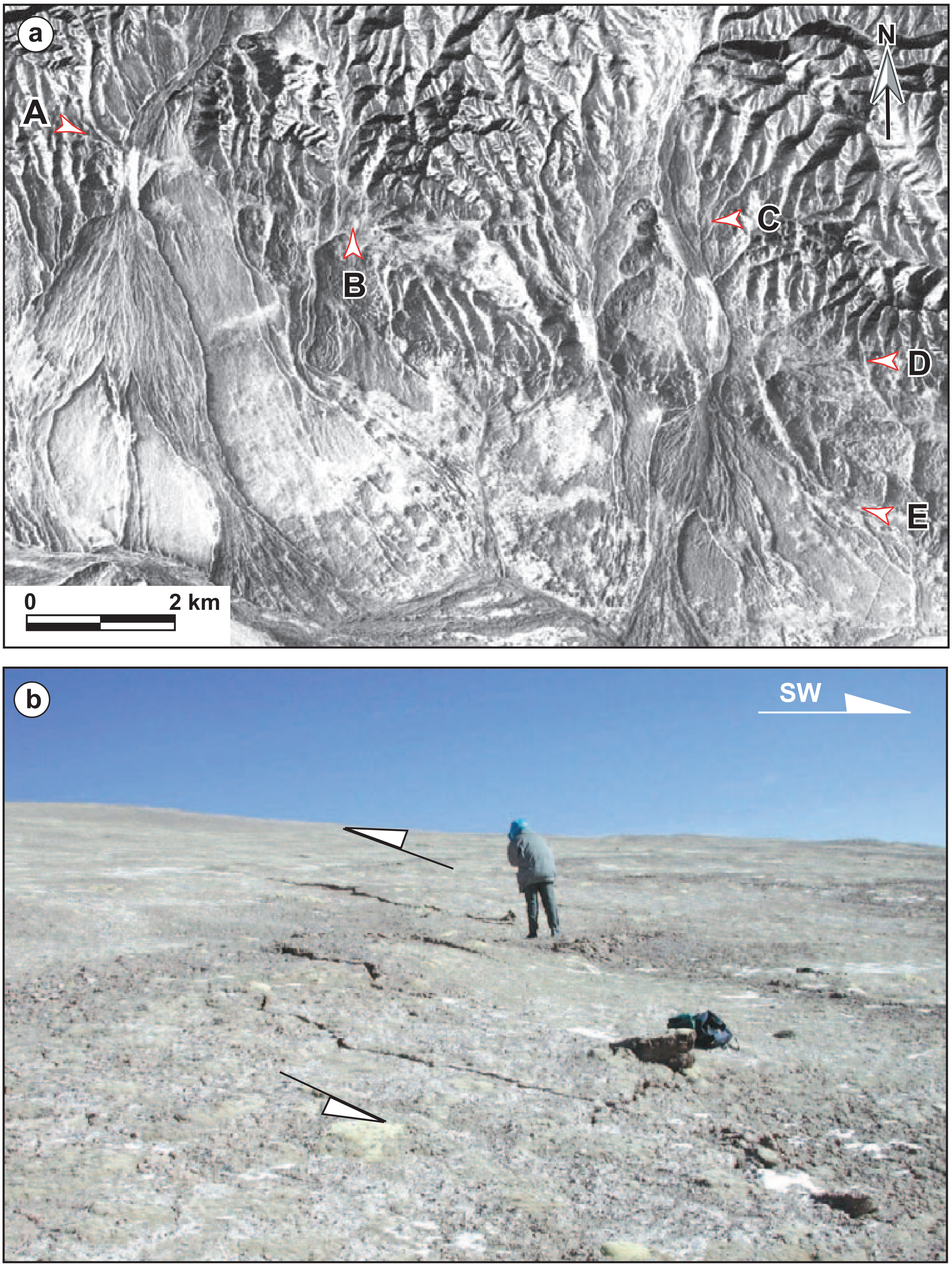

Fig.14. (a) SPOT image (January 25, 2002) showing that the easternmost termination of the 2001 surface rupture zone, appearing as a flat-lying Y-shape pattern. Location is shown on Fig. 13a. (b) Photograph showing that rupture zone gradually disappeared near the easternmost end, where the ruptures appearing an en-echelon pattern. For location see point E in Fig. 14a.

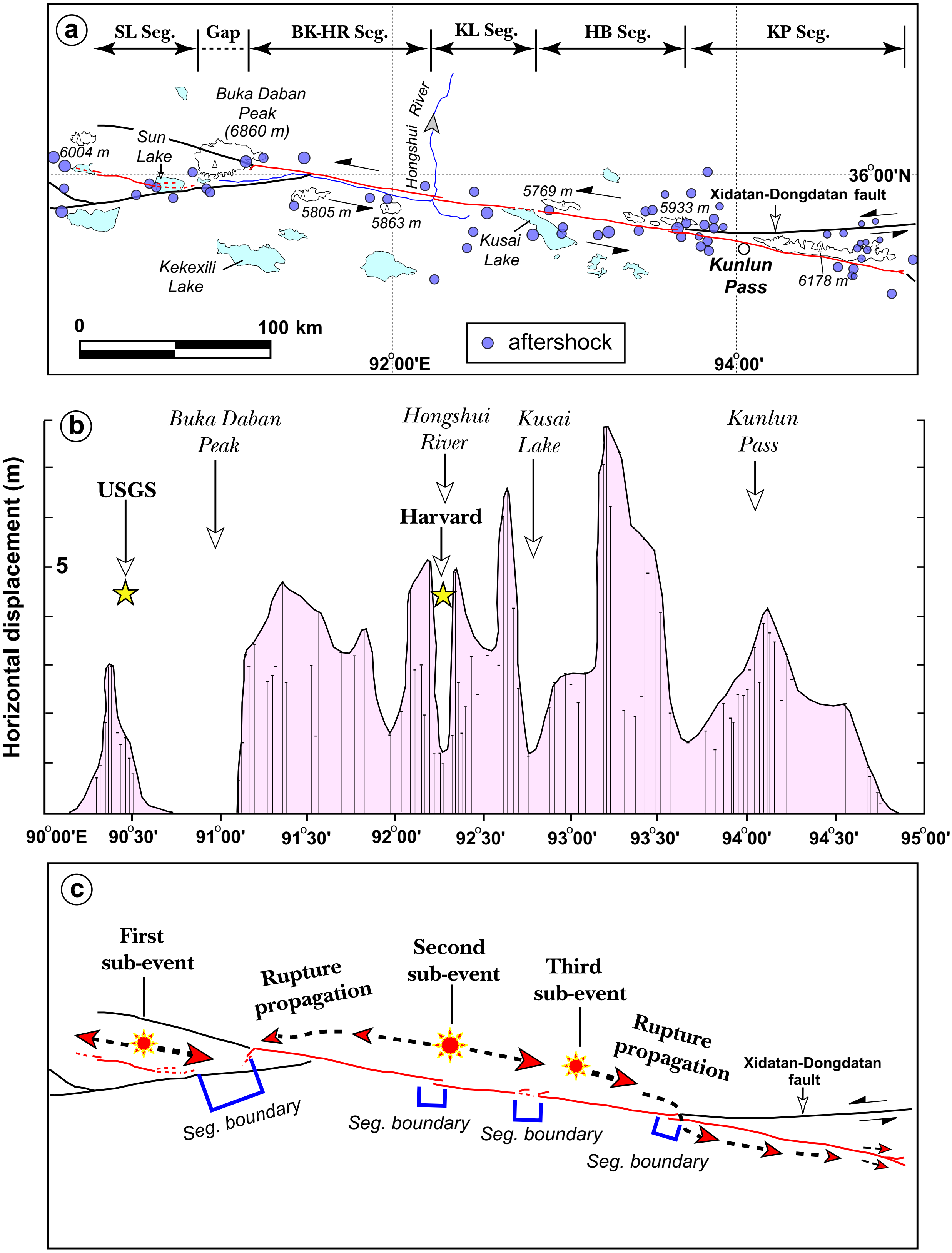

Fig.15. (a) Geometry and segmentation of the surface rupture zone associated with the 2001 large seismic event. The distribution of major aftershocks (M_L>3.0) occurred during 14 November 2001 and 27 November 2001 (modified from Xu and Chen, 2004). (b) Slip distribution along the surface rupture zone, compiled from our field measurements and previous published results (CSB, 2002; Zhao *et al.*, 2002). Locations of three major sub-events are same with the USGS`s epicenter, Harvard Moment Centriod, and third sub-event suggested by Xu and Chen (2004), respectively. (c) Rupture propagation model showing a complex multiple rupture process related to the 2001 seismic event.